Design, Synthesis, Structure−Activity Relationships, and Molecular Modeling Studies of 2,3-Diaryl-1,3-thiazolidin-4-ones as Potent Anti-HIV Agents

ARTICLE *in* JOURNAL OF MEDICINAL CHEMISTRY · DECEMBER 2002

Impact Factor: 5.45 · DOI: 10.1021/jm020977+ · Source: PubMed

12 AUTHORS, INCLUDING:

Maria Letizia Barreca
Università degli Studi di Perugia
74 PUBLICATIONS **1,824** CITATIONS
SEE PROFILE

Hans-Dieter Höltje
Heinrich-Heine-Universität Düsseldorf
188 PUBLICATIONS **2,470** CITATIONS
SEE PROFILE

Anna-Maria Monforte
Università degli Studi di Messina
87 PUBLICATIONS **1,512** CITATIONS
SEE PROFILE

Christophe Pannecouque
University of Leuven
435 PUBLICATIONS **7,261** CITATIONS
SEE PROFILE

Design, Synthesis, Structure−Activity Relationships, and Molecular Modeling Studies of 2,3-Diaryl-1,3-thiazolidin-4-ones as Potent Anti-HIV Agents

Maria L. Barreca,[†] Jan Balzarini,[‡] Alba Chimirri,[†] Erik De Clercq,[‡] Laura De Luca,[†] Hans Dieter Höltje,[§] Monika Höltje,[§] Anna Maria Monforte,[†] Pietro Monforte,[†,*] Christophe Pannecouque,[‡] Angela Rao[†], and Maria Zappalà[‡]

Dipartimento Farmaco-Chimico, Università di Messina, Viale Annunziata, 98168 Messina, Italy; Rega Institute for Medical Research, Katholieke Universiteit Leuven, 10 Minderbroedersstraat, B-3000, Leuven, Belgium; and Institut für Pharmazeutische Chemie, Heinrich-Heine-Universität Düsseldorf, Germany

Received June 24, 2002

Starting from 1*H*,3*H*-thiazolo[3,4-*a*]benzimidazoles (TBZs), we performed the design, synthesis, and the structure−activity relationship studies of a series of 2,3-diaryl-1,3-thiazolidin-4-ones. Some derivatives proved to be highly effective in inhibiting HIV-1 replication at nanomolar concentrations with minimal cytotoxicity, thereby acting as nonnucleoside HIV-1 RT inhibitors (NNRTIs). Computational studies were used to delineate the ligand-RT interactions and to probe the binding of the ligands to HIV-1 RT.

Introduction

Reverse transcriptase (RT) is a key enzyme which plays an essential and multifunctional role in the replication of the human immunodeficiency virus (HIV)[1] and thus represents an attractive target for the development of new drugs useful in AIDS therapy.[2] RT is necessary for the catalytic transformation of single-stranded viral RNA into the double-stranded linear DNA which is integrated into host cell chromosomes.

Nonnucleoside RT inhibitors (NNRTIs) bind in a noncompetitive manner to a unique site on the enzyme, altering its ability to function and achieving a highly selective suppression of HIV-1 replication with little cytotoxicity.[3] X-ray crystallographic studies of NNRTI/RT complexes have shown that the NNRTIs, unlike their structural diversity, present a very similar conformational "butterfly-like" shape.[4] Presently, three NNRTIs, namely nevirapine, delavirdine, and efavirenz are available in clinical practice. Combination of these drugs with nucleoside RT inhibitors and protease inhibitors leads to a dramatic decrease of the viral load in most of the HIV-infected patients. However, in view of the increasing incidence of resistance to current drug regimens and the frequency of adverse events, the development of novel, selective, potent, safe, inexpensive antiviral agents, that are also effective against mutant HIV strains, remains a high priority for medical research.

In previous papers[5] we reported a series of 1-aryl-1*H*,3*H*-thiazolo[3,4-*a*]benzimidazoles (TBZs) (Chart 1), which proved to be highly active as HIV-1 NNRTIs. Extensive structure−activity relationship (SAR) studies were performed, and specific requirements were observed with regard to the structural determinants for optimum anti-HIV activity. The C-1 substituent plays a decisive and crucial role in the interaction of TBZ compounds with the target HIV-1 RT: in particular a 2,6-dihalo-substituted phenyl ring at C-1 gave a large improvement in potency.

Chart 1. Structure of TBZ Derivatives

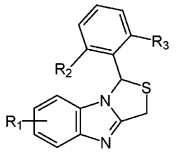

We have also demonstrated, by Comparative Molecular Field Analysis (CoMFA) and flexible docking experiments,[6] that the biological activity of TBZs is associated with their ability to assume a "butterfly-like" conformation, analogously to other NNRTIs. In particular, the plausible pharmacophoric elements for TBZs were found to be the benzene fused ring, the aryl group at C-1, and the nitrogen atom of the thiazole nucleus.

Using the thiazolobenzimidazole system as a scaffold, we designed 2,3-diaryl-1,3-thiazolidin-4-one derivatives as new NNRTIs. The opening of the imidazole nucleus allowed us to keep the main molecular determinants responsible for potent enzyme inhibition. To gain more specific information about the mechanism of action of NNRTIs, computational methods have been used to map the drug−enzyme interaction zones and to identify the correct binding mode of this new class of antiviral agents. A preliminary account of these results has been reported.[7]

Chemistry

The synthesis of the new 2,3-diaryl-1,3-thiazolidin-4-ones (**4**−**34**) was carried out according to reported procedures,[7] by reacting a suitable 2,6-dihalo-substituted benzaldehyde (**3**) with an equimolar amount of a (hetero)aromatic amine (**1**) in the presence of an excess of mercaptoacetic acid (**2**) in refluxing toluene (Scheme 1).

* To whom correspondence should be addressed: Pietro Monforte, Dipartimento Farmaco-Chimico, Viale Annunziata, 98168 Messina. Phone: +39 090 6766520; FAX: +39 090 355613; e-mail: monforte@pharma.unime.it.

[†] Dipartimento Farmaco-Chimico.

[‡] Rega Institute for Medical Research.

[§] Institut für Pharmazeutische Chemie.

10.1021/jm020977+ CCC: $22.00
Published on Web 10/25/2002

Scheme 1

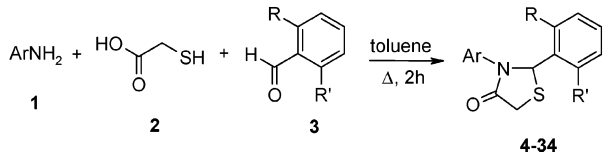

Results and Discussion

Compounds **4**−**34** and TBZ were evaluated for anti-HIV activity by determining their ability to inhibit the replication of HIV-1 (III_B) or HIV-2 (ROD) in MT-4 cells (Table 1). The anti-HIV activity of several derivatives was also measured in HIV-1_{IIIB}-infected CEM cells (Table 2). In Table 2 the inhibitory effects on HIV-1 RT enzymatic activity are also reported. The results obtained show that our approach has led to the development of highly potent anti-HIV-1 agents, up to 10-fold more potent than the TBZ lead compound, probably because the new molecules, being more flexible, are better accommodated into the HIV-1 RT binding pocket. In addition, these compounds were minimally toxic, and their selectivity indices were remarkably high (up to 10000). As observed for other classes of NNRTIs, none of the compounds inhibited the replication of HIV-2 (ROD) in MT-4 cells at subtoxic concentrations.

Compounds **21** and **29**−**31**, among the most potent of the series, were also evaluated against an extensive panel of mutant virus strains that contained single mutation in their RT characteristic for NNRTI resistance (Table 3). All the tested compounds kept antiviral activity against mutant HIV-1 strains, in particular against 100Leu→Ile, 138Glu→Lys mutant viruses.

From a structure−activity relationship viewpoint, the anti-HIV activity was strongly enhanced by introducing a 2-pyridinyl moiety at the N-3 of the thiazolidinone ring and in particular by a 2′,6′-dichlorophenyl substituent at C-2: in fact derivative **8** was more active than its analogues **5** and **10**, while compound **6** was more active than **4** and **9** as well as **7** and **8**. As suggested by molecular modeling studies,[6] the introduction of a lipophilic substituent at the 6 position of the pyridin-2-yl group led to a substantial increase in antiviral activity. In fact, the compounds with the best combination of high potency and low toxicity were 6-substituted-pyridin-2-yl derivatives, such as **20** and **21** and **29**−**34**.

To carry on our previous 3D QSAR analyses, we have performed computational studies of the RT structure in order to better characterize the binding sites of the enzyme and to better understand the determinants for high inhibitory activity. The main intermolecular interactions involved in the RT inhibition were investigated using the GRID program.[8]

To date, several crystal structures of HIV-1 RT in complex with different NNRTIs have been reported, which provide information about the exact location and composition of the nonnucleoside inhibitor binding pocket (NNIBP) and the opportunity to use the enzyme in a functional conformation. We used the X-ray structure of the enzyme from the nevirapine/RT complex (PDB code 1VRT) because the nevirapine is one of the three NNRTIs approved by the FDA and also for the high resolution of this crystal structure (2.2 Å).

With the aim to identify the binding sites complementary to the functional groups of the ligands, several probes with different chemical characteristics were chosen and their atom affinity potentials calculated on a grid that surrounds the allosteric pocket. The most energetically favorable binding zones were detected with the hydrophobic DRY probe (Figure 1, a). The GRID interaction field calculated with this probe indicated a large region in the NNIBP that perfectly corresponds with the location of nevirapine in the complex.

No significant maps were indeed detected for the halogen probes, except for the fluorine whose regions of interaction were almost superimposed on those of the hydrophobic probe. This could be explained by considering that halogen atoms are not crucial for the binding affinity, but influence the correct orientation of the phenyl ring at C-2 allowing molecules to assume the butterfly-like conformation, analogously to what we observed for TBZs by X-ray analysis.[5a]

More specific probes were used in order to gain further insight into the nature of the hydrophobic interactions. GRID method detected favorable binding zones for the aliphatic methyl and aromatic probes. In particular, the three main regions of interaction obtained matched very well with the positions of the methyl group, the pyridine nucleus, and the cyclopropyl substituent of nevirapine in the corresponding X-ray structure (Figure 1b). These results should be taken in account in the design of new NNRTIs; in fact, to have a potent RT inhibitory activity, it might be sufficient to obtain molecules which present, in their bioactive conformation, three nonpolar parts in the exact spatial disposition suggested by the GRID contour maps.

On these bases, we performed docking experiments on our 2,3-diaryl-1,3-thiazolidin-4-ones with the aim to predict their correct binding mode at the RT level, to compare the obtained docked conformations with the GRID molecular interaction fields and finally to obtain information for the design of new potential NNRTIs.

Using again as macromolecule target the X-ray structure of the enzyme from nevirapine/RT complex, an automated molecular docking procedure using the AutoDock program was performed.[9] To validate the ability of the method, a docking study of nevirapine was carried out, and the program perfectly reproduced the experimental position of the ligand (80 runs of 100, with a binding energy of −10.87 kcal/mol). Then, the two most active compounds of the series, compounds **21** and **29**, were chosen as ligand, and the results were superimposed with the nevirapine bound to the RT.

Compound **21** clearly preferred a single binding position in the allosteric pocket (42 runs of 100, with a binding energy of −9.71 kcal/mol) (Figure 2, a), which is the best prediction since it has the lowest energy among the clusters. Comparison of the X-ray structure of nevirapine with **21** showed that the following parts of these molecules are perfectly overlapped: the 3-(6-bromopyridin-2-yl) group, the 2-(2,6-difluorophenyl) ring and the CH_2−S moiety of the thiazolidin-4-one nucleus of compound **21** are superimposed to 4-methylpyridine, the other pyridine nucleus, and the cyclopropyl substituent of nevirapine, respectively. In such orientation, the bound conformation of **21** presents a good degree of steric overlap with the experimental position of nevirapine and is involved in van der Waals contacts with the residues surrounding the NNIBP.

Table 1. Anti-HIV-1 Activity, Cytotoxicity, and Selectivity Index in MT-4 Cells for Compounds **4**−**34**

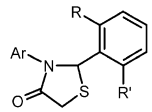

compd	Ar	R	R′	EC_{50} (μM)[a]	CC_{50} (μM)[b]	SI[c]
4	phenyl	Cl	Cl	0.401 ± 0.093	38.1 ± 4.5	95
5	phenyl	F	F	2.30 ± 0.75	>429	>186
6	pyridin-2-yl	Cl	Cl	0.178 ± 0.009	38.5 ± 4.9	216.3
7	pyridin-2-yl	Cl	F	0.278 ± 0.055	41.7 ± 1.6	150
8	pyridin-2-yl	F	F	0.855 ± 0.068	>427	>500
9	pyridin-3-yl	Cl	Cl	NA	23.4 ± 6.9	-
10	pyridin-3-yl	F	F	95.1 ± 65.3	>427	>4.5
11	pyridin-4-yl	Cl	Cl	NA	10.0 ± 3.5	-
12	pyridin-4-yl	F	F	NA	33.9 ± 0.5	-
13	5-Cl-pyridin-2-yl	Cl	Cl	1.78 ± 0.53	19.2 ± 2.6	11
14	5-Cl-pyridin-2-yl	Cl	F	2.13 ± 0.82	29.4 ± 6.7	14
15	5-Cl-pyridin-2-yl	F	F	7.19 ± 0.12	29.8 ± 1.1	4.2
16	5-Br-pyridin-2-yl	Cl	Cl	1.51 ± 0.22	28.2 ± 13.6	18.6
17	5-Br-pyridin-2-yl	Cl	F	1.24 ± 0.10	30.7 ± 2.3	25
18	5-Br-pyridin-2-yl	F	F	4.85 ± 0.48	36.1 ± 11.3	7.4
19	6-Br-pyridin-2-yl	Cl	Cl	0.272 ± 0.025	67.4 ± 37.7	248
20	6-Br-pyridin-2-yl	Cl	F	0.064 ± 0.0	30.7 ± 1.5	484
21	6-Br-pyridin-2-yl	F	F	0.030 ± 0.013	32.0 ± 0.54	1066
22	3-Me-pyridin-2-yl	Cl	Cl	NA	42.6 ± 4.8	-
23	3-Me-pyridin-2-yl	F	F	53.5 ± 39.1	>319.3	>6
24	4-Me-pyridin-2-yl	Cl	Cl	0.147 ± 0.050	>368.5	>2500
25	4-Me-pyridin-2-yl	Cl	F	0.099 ± 0.037	33.9 ± 0.9	343
26	4-Me-pyridin-2-yl	F	F	0.248 ± 0.026	242.2 ± 0.3	976
27	5-Me-pyridin-2-yl	Cl	Cl	1.41 ± 0.15	24.9 ± 0.62	17.7
28	5-Me-pyridin-2-yl	F	F	5.13 ± 0.0	201.6 ± 36.7	39.3
29	6-Me-pyridin-2-yl	Cl	Cl	0.044 ± 0.003	284.7 ± 33.6	6470
30	6-Me-pyridin-2-yl	Cl	F	0.053 ± 0.009	31.9 ± 2.0	601
31	6-Me-pyridin-2-yl	F	F	0.082 ± 0.029	126.0 ± 34.9	1536
32	4,6-di-Me-pyridin-2-yl	Cl	Cl	0.090 ± 0.037	64.1 ± 71.1	712
33	4,6-di-Me-pyridin-2-yl	Cl	F	0.042 ± 0.003	41.6 ± 4.7	986
34	4,6-di-Me-pyridin-2-yl	F	F	0.059 ± 0.012	43.4 ± 2.9	735
TBZ				0.352 ± 0.14	19.2 ± 2.8	54.5

[a] Concentration required to reduce HIV-1-induced cytopathic effect by 50% in MT-4 cells. [b]Concentration required to reduce MT-4 cell viability by 50%. [c] Selectivity index: ratio CC_{50}/EC_{50}. NA = not active.

Table 2. Anti-HIV-1 Activity, Cytotoxicity, and Selectivity Index in CEM Cells and RT Inhibitory Activity for Some 2,3-Diaryl-1,3-thiazolidin-4-ones

compd	EC_{50} (μM)[a]	CC_{50} (μM)[b]	SI[c]	RT data[d]
7	0.242 ± 0.022	191.4 ± 85.2	791	
12	NA	284.4 ± 11.8	-	NA
13	1.86 ± 0.78	31.1 ± 3.3	17	
15	4.13 ± 0.64	47.1 ± 11.3	11	67.0 ± 7.04
16	1.31 ± 0.57	26.0 ± 0.0	20	56.6 ± 1.48
18	2.50 ± 1.37	45.8 ± 7.5	18	61.4 ± 4.31
19	0.173 ± 0.035	≥247.5	≥1431	
21	0.030 ± 0.002	≥269.4	≥8980	0.91 ± 0.16
25	0.108 ± 0.065	56.7 ± 5.3	525	4.12 ± 0.62
26				2.84 ± 0.39
27	1.32 ± 0.94	31.2 ± 0.62	24	42.4 ± 1.77
29				2.24 ± 0.38
30	0.040 ± 0.012	44.3 ± 3.7	1108	2.85 ± 0.49
31				2.90 ± 0.49
32	0.130 ± 0.057	≥283.1	≥2178	
34	0.078 ± 0.031	≥62.4	≥800	4.12 ± 0.25
TBZ	1.10 ± 0.32	50.0 ± 3.2	45	14.6 ± 2.6

[a] Concentration required to reduce HIV-1-induced cytopathic effect by 50% in CEM cells. [b]Concentration required to reduce CEM cell viability by 50%.[c]Selectivity index: ratio CC_{50}/EC_{50}. [d]IC_{50} (μM); poly(rC)/oligo(dG) was used as the template/primer and [^{3}H]dGTP as the radiolabeled substrate. NA = not active.

For compound **29** most of the results were found in the top two clusters (32 in the top cluster and 15 in the cluster ranked second), so two different orientations were taken in account as mode of interaction for this ligand (Figure 2b). The most favorable result (binding energy −10.74 kcal/mol) presents this ligand in the same position as observed for molecule **21**. An alternative to this binding mode is given by the second cluster, which is found less frequently but shows a binding energy (−9.74 kcal/mol) similar to the first one. In this orientation, the 3-(6-methylpyridin-2-yl) group of **29** is situated in the same area as the cyclopropyl substituent of nevirapine, the 2-(2,6-dichlorophenyl) ring overlaps with the pyridine nucleus and the 1,3-thiazolidin-4-one lies in the same position as the 4-methylpyridine. The results indicate that the functional groups of similar chemical character are placed in similar ways and show comparable interactions with the RT protein. Thus, both conformations of **29** might represent a reasonable potential binding mode at the NNIBP.

The relative docked orientations of derivatives **21** and **29** were then superimposed to the GRID interaction fields calculated with the aliphatic methyl and aromatic probes and, as pointed out in Figure 3, showed a suitable fit with the three zones identified in the RT enzyme, confirming a very good alignment of the major structural features of 2,3-diaryl-1,3-thiazolidin-4-ones with other known NNRTIs, such as nevirapine.

On these bases, we are now pursuing the synthesis of new 2,3-diaryl-1,3-thiazolidin-4-one derivatives, in which an improvement of the anti-HIV activity could be obtained by increasing the lipophilic characteristics

Table 3. Anti-HIV-1 Activity of Compounds **21** and **29**−**31** against Mutant HIV-1 Strains in CEM Cells

	EC_{50} (μM)[a]					
compd	HIV-1_{IIIB}	100 Leu→Ile	103 Lys→Asn	138 Glu→Lys	181 Tyr→Cys	188 Tyr→His
21	0.026 ± 0.018	0.94 ± 0.18	≥11	0.073 ± 0.089	1.88 ± 1.07	1.02 ± 0.83
29	0.073 ± 0.029	0.150 ± 0.079	≥ 60	0.117 ± 0.117	-	16.2 ± 6.2
30	0.031 ± 0.015	0.102 ± 0.074	10.5 ± 2.8	0.124 ± 0.124	7.28 ± 0.65	4.64 ± 0.00
31	0.117 ± 0.019	0.75 ± 0.32	35.9 ± 2.28	0.39 ± 0.19	≥13	≥13
TBZ	1.39 ± 0.56	3.12 ± 0.94	15.6 ± 3.2	1.73 ± 1.02	13.8 ± 4.2	4.16 ± 1.12

[a] Concentration required to protect CEM cells against the HIV-induced cytopathogenicity by 50%.

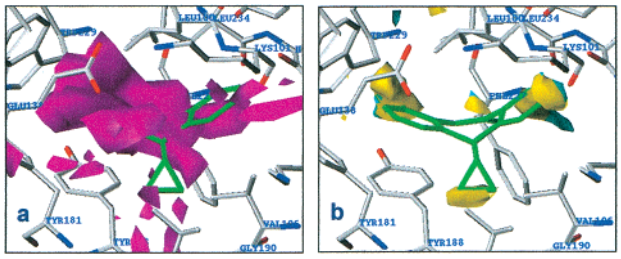

Figure 1. GRID contour maps calculated using the hydrophobic (purple, **a**), the aliphatic methyl (yellow) and the aromatic (cyan) probes (**b**) in the NNRTI binding site. In both pictures nevirapine is shown in green.

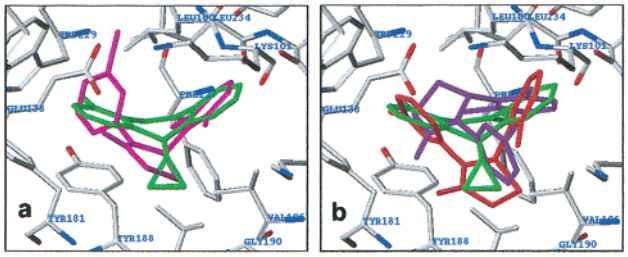

Figure 2. Superimposition of the docked conformations of compounds **21** (magenta, **a**) and **29** (top and second-ranked, red and purple, **b**) over the crystal structure orientation of nevirapine (green).

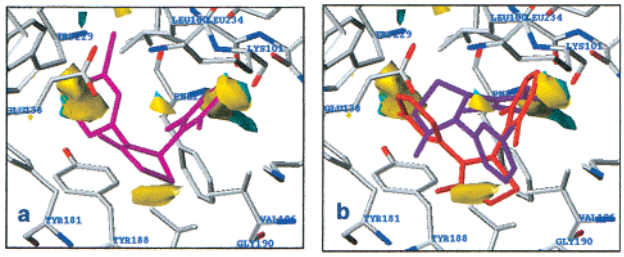

Figure 3. Comparison of the location of compounds **21** (magenta, **a**) and **29** (red and purple, **b**) in the NNBP and GRID interaction fields calculated with the aliphatic methyl (yellow) and the aromatic (cyan) probes.

both of the substituent at N-3 and by changing some structural features also in thiazolidinone nucleus.

Conclusions

Starting from previously described 1*H*,3*H*-thiazolo[3,4-*a*]benzimidazoles, we designed and synthesized a new series of 2,3-diaryl-1,3-thiazolidin-4-ones which proved to be potent and selective NNRTIs. Computational studies were also carried out with the aim to find the most energetically favorable binding sites involved in RT inhibition. The GRID approach allowed the detection of three lipophilic regions within the NNIBP as determinants for high inhibitory activity. Moreover, an automated molecular docking approach suggested that the binding mode of these compounds is similar to that observed for other NNRTIs in their experimental positions in the allosteric RT binding site.

Acknowledgment. These investigations were supported in part by the Ministero dell'Istruzione, dell'Università e della Ricerca (COFIN 2000, Rome, Italy), and in part by the Flemish Fonds voor Wetenschappelijk Onderzoek (FWO Grant G.0104.98) and the Belgian Geconcerteerde Onderzoeksacties (GOA 00/12). We thank ISEP/FORTIS for financial support and Kristien Erven for excellent technical assistance.

Supporting Information Available: Physical and spectral data of all the synthesized compounds, experimental procedure for synthesis, molecular modeling studies, and anti-HIV activity evaluation. This material is available free of charge via the Internet at http//pubs.acs.org.

References

(1) Jonckheere, H.; Anné, J.; De Clercq, E. The HIV-1 reverse transciption (RT) process as target for RT inhibitors. *Med. Res. Rev.* **2000**, *20*, 129−154.

(2) De Clercq, E. Novel compounds in preclinical/early clinical development for the treatment of HIV infections. *Rev. Med. Virol.* **2000**, *10*, 255−277.

(3) Hajos, G.; Riedi, S.; Molnar, J.; Szabo, D. Nonnucleoside reverse transcriptase inhibitors. *Drugs Fut.* **2000**, *25*, 47−62.

(4) Schäfer, W.; Friebe, W.-G.; Leinert, Mertens, A.; Poll, T.; von der Saal, W.; Zilch, H.; Nuber, H.; Ziegler, M. L.; Nonnucleoside inhibitors of HIV-1 reverse transcriptase: molecular modeling and X-ray structure investigations. *J. Med. Chem.* **1993**, *36*, 726−732.

(5) (a) Chimirri, A.; Grasso, S.; Molica, C.; Monforte, A. M.; Monforte, P.; Zappalà, M.; Bruno, G.; Nicolò, F.; Witvrouw, M.; Jonckeere, H.; Balzarini, J., De Clercq, E. Structural features and anti-human immunodeficiency virus (HIV) activity of the isomers of 1-(2′,6′-difluorophenyl)-1*H*, 3*H*-thiazolo[3,4-*a*]benzimidazole, a potent nonnucleoside HIV-1 reverse transcriptase inhibitor. *Antiv. Chem. Chemother.* **1997**, *8*, 363−370. (b) Chimirri, A.; Grasso, S.; Monforte, A. M.; Monforte, P.; Rao, A.; Zappalà, M.; Bruno, G.; Nicolò, F.; Pannecouque, C.; Witvrouw, M.; De Clercq, E. Synthesis, structure and in vitro anti-human immunodeficiency virus activity of novel 3-methyl-1*H*,3*H*-thiazolo[3,4-*a*]-benzimidazoles. *Antiv. Chem. Chemother.* **1998**, *9*, 431−438. (c) Chimirri, A.; Grasso, S.; Monforte, P.; Rao, A.; Zappalà, M.; Monforte, A. M.; Pannecouque, C.; Witvrouw, M.; Balzarini, J.; De Clercq, E. Synthesis and biological activity of novel 1*H*,3*H*-thiazolo[3,4-*a*]benzimidazoles: nonnucleoside human immunodeficiency virus type 1 reverse transcriptase inhibitors. *Antiv. Chem. Chemother.* **1999**, *10*, 211−217.

(6) Barreca, M. L.; Chimirri, A.; Carotti, A.; Carrieri, A.; Monforte, A. M.; Pellegrini Calace, M.; Rao, A. Comparative Molecular Field Analysis (CoMFA) and docking studies of nonnucleoside HIV-1 RT inhibitors (NNRTIs). *Bioorg. Med. Chem.* **1999**, *7*, 2283−2292.

(7) Barreca, M. L.; Chimirri, A.; De Luca, L.; Monforte, A. M.; Monforte, P.; Rao, A.; Zappalà, M.; Balzarini, J.; De Clercq, E.; Pannecouque, C.; Witvrouw, M. Discovery of 2,3-diaryl-1,3-thiazolidin-4-ones as potent anti-HIV-1 agents. *Bioorg. Med. Chem. Lett.* **2001**, *11*, 1793−1796.

(8) Goodford P. J. A computational procedure for determining energetically favorable binding sites on biologically important macromolecules. *J. Med. Chem.* **1985**, *28*, 849−857.

(9) Morris, G. M.; Goodsell, D. S.; Halliday, R. S.; Huey, R.; Hart, W. E.; Belew R. K.; Olson, A. J. Automated docking using a Lamarckian genetic algorithm and an empirical binding free energy function. *J. Comput. Chem.* **1998**, *19*, 1639−1662.

JM020977+